ELSEVIER

Ceramics International 30 (2004) 2183–2189

CERAMICS INTERNATIONAL

www.elsevier.com/locate/ceramint

Synthesis, formation and characterization of $ZnTiO_3$ ceramics

Yee-Shin Chang [a], Yen-Hwei Chang [a,*], In-Gann Chen [a], Guo-Ju Chen [b], Yin-Lai Chai [c], Te-Hua Fang [d], Sean Wu [e]

[a] *Department of Materials Science and Engineering, National Cheng Kung University, Tainan 701, Taiwan, ROC*
[b] *Department of Material Science and Engineering, I-Shou University, Kaohsiung 840, Taiwan, ROC*
[c] *Department of Resources Engineering, Dahan Institute of Technology, Hualien 971, Taiwan, ROC*
[d] *Department of Mechanical Engineering, Southern Taiwan University of Technology, Tainan 710, Taiwan, ROC*
[e] *Department of Electronics and Information Engineering, Tung-Fang Institute of Technology, Kaohsiung 821, Taiwan, ROC*

Received 5 September 2003; received in revised form 2 January 2004; accepted 29 January 2004
Available online 14 April 2004

Abstract

Zinc titanate ($ZnTiO_3$) powders of perovskite structure were synthesized by conventional solid state reaction using metal oxides. Powders of ZnO and TiO_2 in a molar ratio of 1:1 were mixed in a ball mill and then heated at temperatures from 700 to 1000 °C for various time periods in air. The crystallization temperature of $ZnTiO_3$ powder was ~820 °C, activation energy for crystallization was ~327.14 kJ/mol and for grain growth was ~48.84 kJ/mol. A transition point was observed when the electrical resistivity was measured versus temperature. Like some ferroelectric materials, a PTCR behavior above the transition temperature was observed with Curie temperature of ~5 °C.

Keywords: A. Powders: solid state reaction; C. Dielectric properties; C. Electrical properties; D. Perovskites

1. Introduction

Fundamental studies concerning the phase diagram and the characterization of the ZnO–TiO_2 system have been published by Dulin and Rase [1] and Bartram and Slepetys [2] since 1960s. They reported that there are three compounds existing in the ZnO–TiO_2 system including α-Zn_2TiO_4 (cubic), Zinc titanate ($ZnTiO_3$, hexagonal), and $Zn_2Ti_3O_8$ (cubic). $ZnTiO_3$ was of a perovskite type oxide structure and could be a useful candidate as microwave resonator [3], gas sensor [4] (for ethanol, NO, CO, etc.), and paint pigment. In addition, $ZnTiO_3$ doped with some transition metal ions could be applied in luminescent purposed by Wang et al. [5,6]. Yamaguchi et al. [7] clarified that $Zn_2Ti_3O_8$ is a low-temperature form of $ZnTiO_3$. Zn_2TiO_4 can be easily prepared by the conventional solid state reaction between 2ZnO and 1TiO_2. Nevertheless, the preparation of pure $ZnTiO_3$ from a mixture of 1ZnO and 1TiO_2 has not been successful because the compound decomposes into α-Zn_2TiO_4 and rutiles at about 945 °C. There are several methods to prepare $ZnTiO_3$ powder including solid state reaction [1], sol–gel [7,8], etc. Zinc titanate nano-crystalline powders prepared by the sol–gel technique have been reported by our earlier study [8] but the processes are generally complicated and the reagents used are very expensive. In this study, the authors have attempted to synthesize $ZnTiO_3$ powders by conventional solid state reaction which is simpler to operate and which uses cheap and easily available oxides as starting materials. The kinetic behavior of the reaction and the characteristics of the resulting $ZnTiO_3$ powders were examined.

2. Experimental

2.1. Powders preparation

The $ZnTiO_3$ powders were prepared by conventional solid state reaction using 99.99% pure ZnO and TiO_2 powders as the starting materials (Aldrich, USA). Even though the starting materials are not very sensitive to moisture, the handling of chemicals was carried out in dry N_2 atmosphere. The starting materials were mixed in ethanol by ball milling for 24 h with zirconia balls in polyethylene jars and dried at 120 °C. Four calcination temperatures were selected to

* Corresponding author. Tel.: +886-6-2757575x62941; fax: +886-6-2382800.
E-mail address: enphei@mail.ncku.edu.tw (Y.-H. Chang).

0272-8842/$30.00 © 2004 Elsevier Ltd and Techna S.r.l. All rights reserved.
doi:10.1016/j.ceramint.2004.01.002

investigate the reaction of formation of zinc titanate: 700, 800, 900, and 1000 °C, respectively, all for 24 h. After having established the optimum calcination temperature, alternative times of 12, 24, 48, and 72 h were applied at that temperature. Before measuring their properties, the powders were pressed at ~50 kg/cm^2 into discs of 10 mm in diameter, 5 mm thickness, and 1.6 g weight. Then, the discs were sintered at temperatures of 800–940 °C for 24 h.

2.2. Characterizations

Powders were analyzed for crystalline structure by X-ray diffractometry (XRD, Rigaku) using Cu Kα radiation to identify the possible phases formed after heat treatment. The average grain sizes of powders were calculated according to the Scherrer's equation. The surface morphology was examined by scanning electron microscopy (HR-SEM, S4200, Hitachi). Differential scanning calorimetry measurements were carried out in an HT-DSC (DSC, Model 404, Netzsch Inc., Exton, PA) equipment in order to investigate the $ZnTiO_3$ phase formation and calculate the activation energies of powders transforming from amorphous to the crystalline state using Kissinger's equation. Samples of about 2–3 mg were placed inside the closed platinum cups. The measurements were carried out with temperature rise at 10, 20, 30, and 40 °C/min, respectively, in a dry nitrogen (99.99%) atmosphere. The calibration was performed using gold as the standard. Temperature dependence of dielectric constant was measured with an inductance–capacitance–resistance (LCR) (Hewlett-Packard, HP-4284A) meter at 1 kHz during the heating and cooling of the sample at 4 °C/min. The electric resistivity was measured between 0 and 40 °C using a multimeter (Hewlett-Packard, HP-3457A).

3. Results and discussion

3.1. Crystallization behavior of $ZnTiO_3$ powders

Fig. 1 shows the XRD patterns of the ZnO and TiO_2 powder mixtures calcined at various temperatures. At 700 °C, there are some peaks of $ZnTiO_3$ shown in the pattern but the peak intensity is low and some intermediate phases are formed. In the pattern of the mixture calcined at 800 °C for 24 h, no peaks of the starting samples can be observed and all peaks were assigned to the hexagonal $ZnTiO_3$ phase with lattice constants: $a = 5.077$ Å, and $c = 13.92$ Å (JCPDS No. 14-0033). Fig. 2 shows the XRD profiles of $ZnTiO_3$ powders after heat treatment at 800 °C for (a) 12 h, (b) 24 h, and (c) 48 h. Single phase $ZnTiO_3$ was observed for various calcination times, however, the intensity of $ZnTiO_3$ peaks increased with increasing time. When calcined for 48 h, traces of α-Zn_2TiO_4 and rutile phases appeared. This may be caused by the reduction of zinc oxide to volatile elemental zinc resulting in a deficiency of zinc in $ZnTiO_3$ which thus becomes sub-stoichiometric and decomposed.

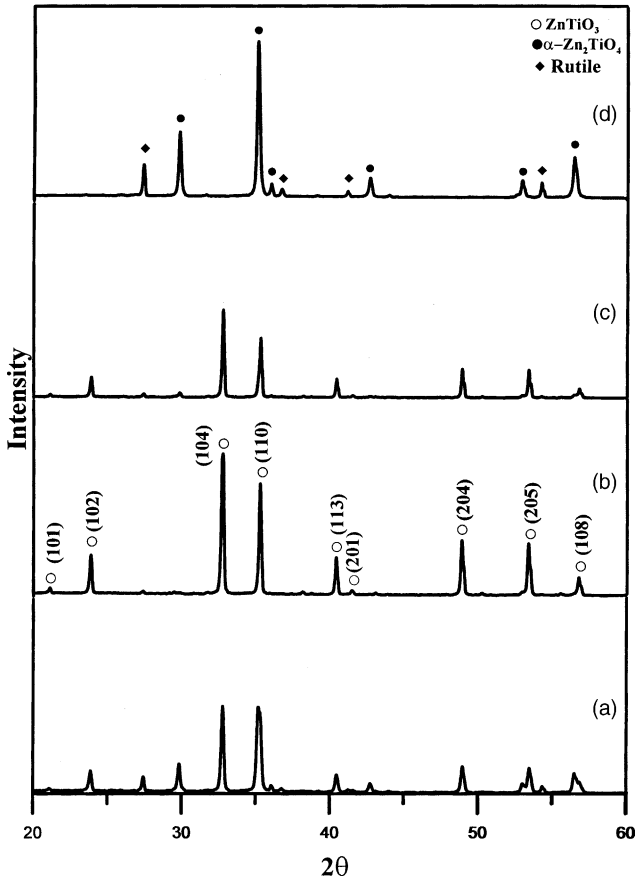

Fig. 1. XRD profiles of $ZnTiO_3$ powder calcined at (a) 700 °C, (b) 800 °C, (c) 900 °C, and (d) 1000 °C for 24 h in air.

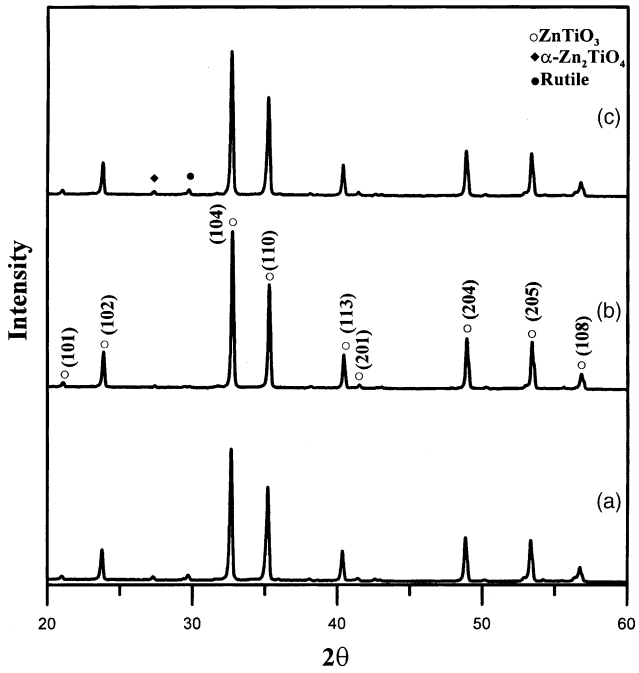

Fig. 2. XRD profiles of $ZnTiO_3$ powder calcined at 800 °C for (a) 12 h, (b) 24 h, and (c) 48 h.

3.2. Average grain sizes and activation energy of grain growth of $ZnTiO_3$ powders

The average grain sizes were determined from XRD powder pattern according to the Scherrer's equation [9]

$$D = \frac{k\lambda}{\beta \cos\theta} \quad (1)$$

where D is the average grain size, k is a constant equal to 0.9, λ is the X-ray wavelength equal to 0.1542 nm, and β is half the peak width. The average grain sizes of powders calcined at 700, 800, and 900 °C were about 540, 700, and 900 nm, respectively. According to Coble's theory [10], the activation energy of grain growth during powder sintering can be calculated by an Arrhenius equation

$$\frac{\mathrm{d}\ln K}{\mathrm{d}T} = \frac{Q}{RT^2} \quad (2)$$

where K is the specific reaction rate constant, Q is the activation energy, T is the absolute temperature, and R is the ideal gas constant.

Bolen and co-workers showed that the value of K is related with grain size directly [11]. Thus integral of Eq. (2) becomes

$$\log D = \left(\frac{-Q}{2.303R}\right)\frac{1}{T + A} \quad (3)$$

where D is the grain size and A is the intercept.

From Eq. (3), by making a plot of log D versus the reciprocal of absolute temperature ($1/T$), a straight-line was obtained as shown in Fig. 3. The slope of the resulting Arrhenius plot is $-Q/(2.303R)$ and the activation energy of grain growth can be obtained and the value of Q is about 48.84 kJ/mol.

3.3. DSC analysis of $ZnTiO_3$ powders

Fig. 4 gives the curves of DSC analysis of $ZnTiO_3$ powders heated at different heating rates of (a) 10 °C/min, (b) 20 °C/min, (c) 30 °C/min, and (d) 40 °C/min, respectively. At a heating rate of 10 °C/min, there appears an endothermic peak near 820 °C showing the formation of $ZnTiO_3$ crystalline phase. This endothermic peak shifts to higher temperatures with increasing heating rate. The temperature was higher than that for the powder prepared by the sol–gel technique [8], this possibly being related to the larger grain size produced by the solid state reaction than for the sol–gel technique. The crystallization activation energy of $ZnTiO_3$ powders was calculated from the relationships of different heating rate versus the endothermic peak value by using the Kissinger's equation [12]

$$\ln\left(\frac{\beta}{T_\mathrm{p}^2}\right) = -\frac{Q}{RT_\mathrm{p}} + C \quad (4)$$

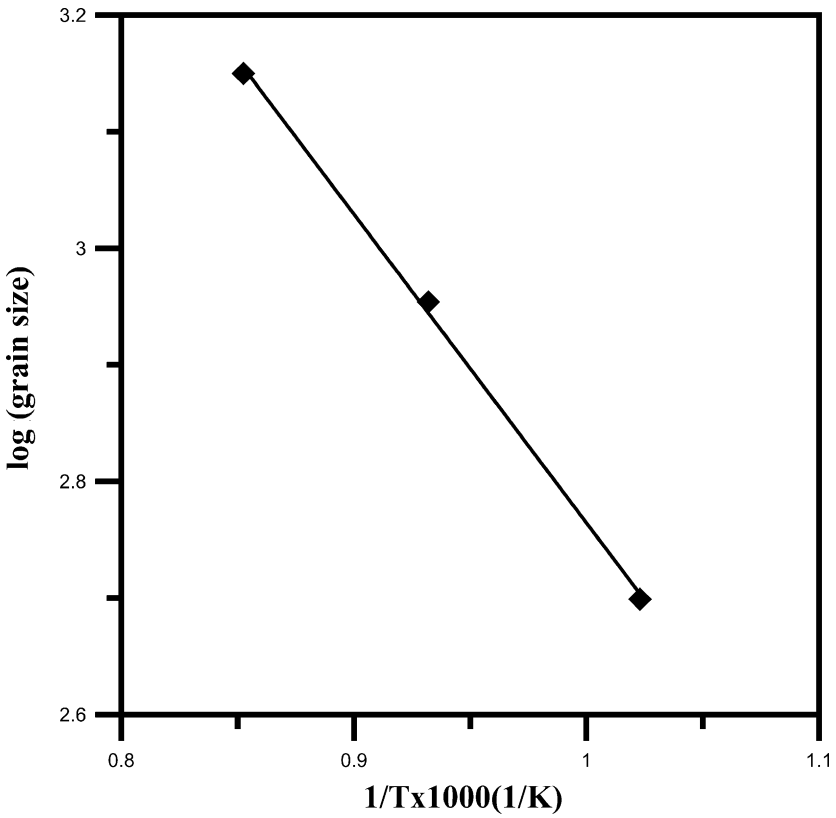

Fig. 3. Plot of log(grain size) vs. $1/T \times 1000$.

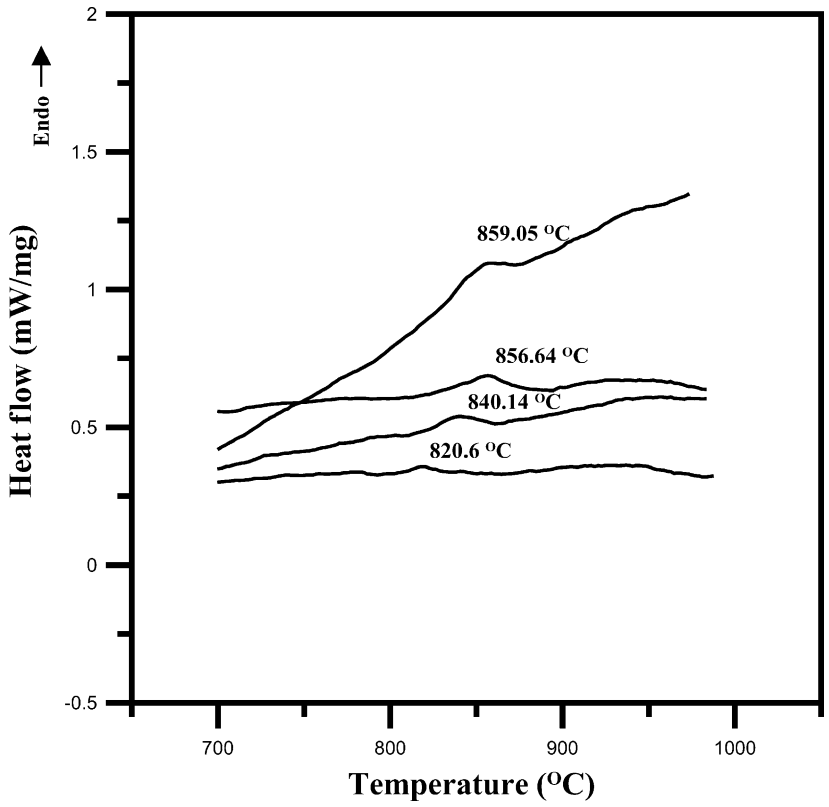

Fig. 4. DSC curves of $ZnTiO_3$ powders obtained at different heating rates of (a) 10 °C/min, (b) 20 °C/min, (c) 30 °C/min, and (d) 40 °C/min.

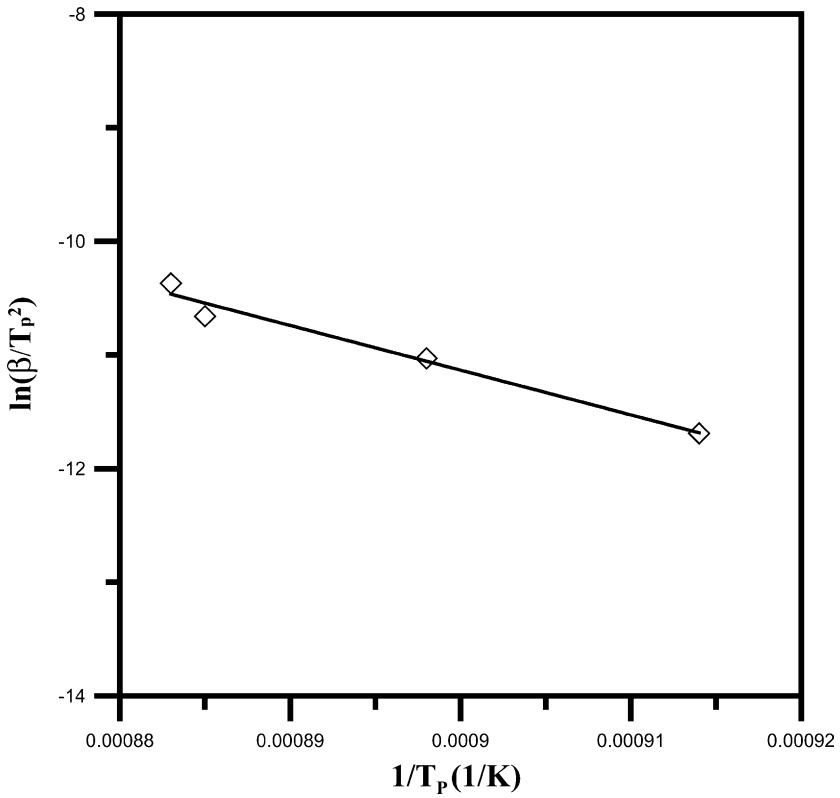

Fig. 5. Plot of $\ln(\beta/T_p^2)$ vs. $1/T_p$.

where β is the heating rate, T_p is the temperature of the endothermic peak, R is the ideal gas constant which equals to 8.314 J/mol, Q is the activation energy, and C is a constant. Making a plot of $\ln(\beta/T_p^2)$ versus the reciprocal of absolute temperature ($1/T_p$) as shown in Fig. 5, the activation energy of crystallization of $ZnTiO_3$ is shown to be 327.14 kJ/mol which is larger than the one resulting for $ZnTiO_3$ crystallization from the sol–gel technique [8].

3.4. SEM micrographs of $ZnTiO_3$ powders

Fig. 6 shows the SEM micrographs of $ZnTiO_3$ powders calcined at different temperatures: (a) 700 °C, (b) 800 °C, and (c) 900 °C for 24 h in air. The sphere like particles seemed to distribute homogeneously, and the particle size increases with the increase in the calcination temperature (the particle size is about 0.5–1 μm for calcination temperatures from 700 to 900 °C). It is believed that a higher temperature enhanced higher atomic mobility and caused

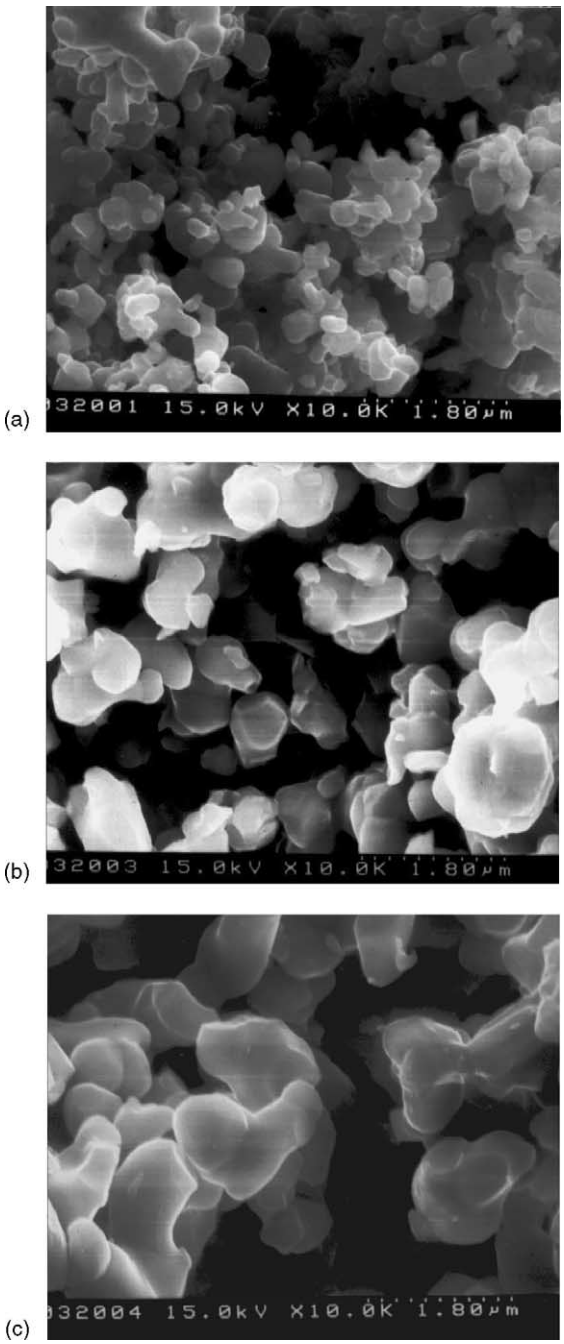

Fig. 6. SEM micrographs of $ZnTiO_3$ powders calcined at (a) 700 °C, (b) 800 °C, and (c) 900 °C for 24 h in air.

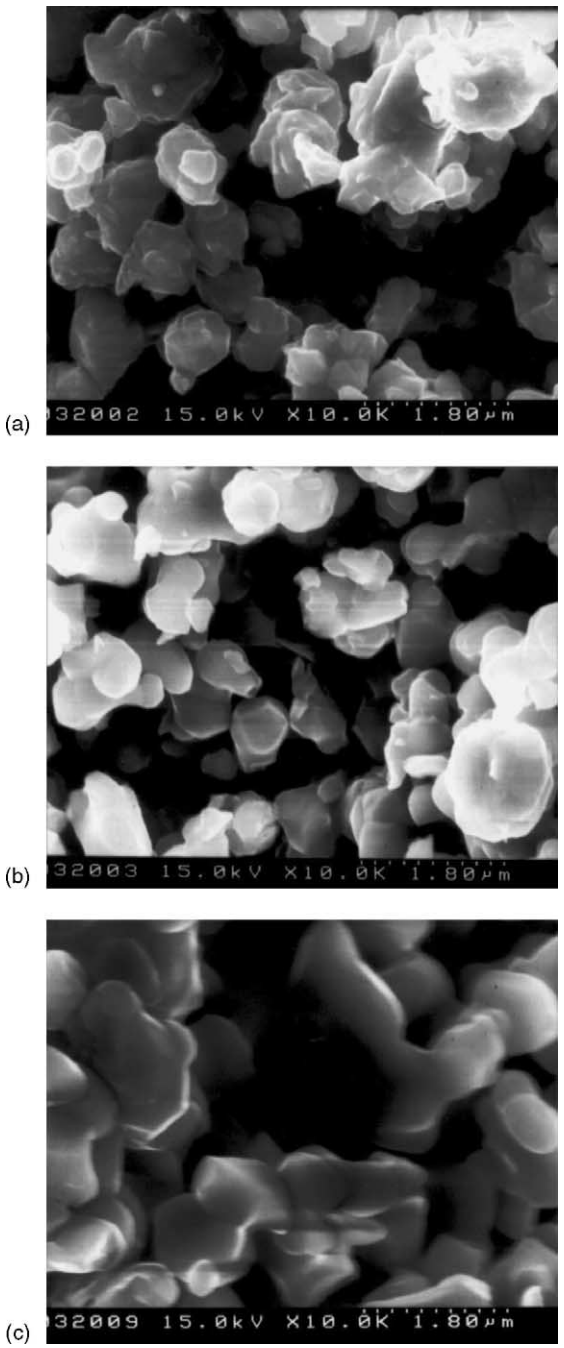

Fig. 7. SEM micrographs of $ZnTiO_3$ powders calcined at 800 °C for (a) 24 h, (b) 48 h, and (c) 72 h in air.

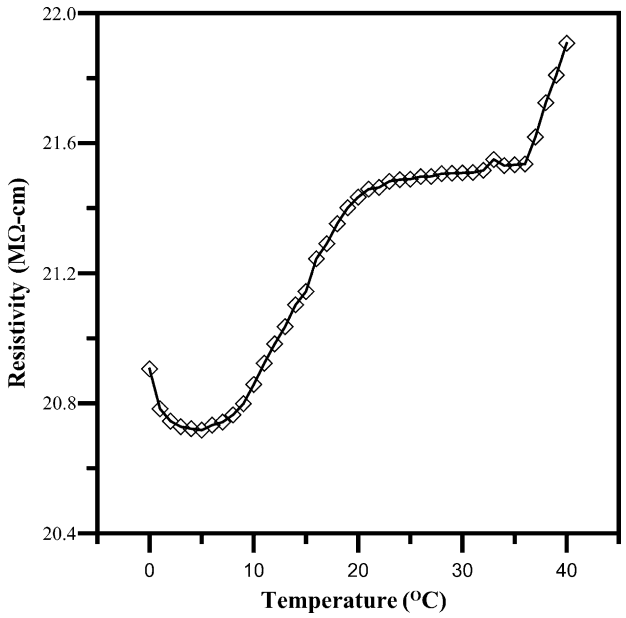

Fig. 8. Temperature dependence of electrical resistivity for $ZnTiO_3$ sintered at 900 °C.

faster grain growth, thus resulting in better crystallinity as confirmed by the X-ray diffraction analysis. Fig. 7 shows the SEM micrographs of $ZnTiO_3$ powders calcined at 800 °C for (a) 12 h, (b) 24 h, and (c) 48 h in air. The size of particles appears to increase with the increase in calcination time. As discussed earlier, the longer calcination time tends to promote phase formation and grain growth.

3.5. Electrical resistivities

ABO_3 perovskite type structure possesses semiconducting behavior. Some semiconducting materials exhibit anomalously strong (exponential) increase in the resistivity ρ with temperature T near the ferroelectric Curie temperature, T_c. This anomalous behavior (of ρ) is well-known as the positive temperature coefficient of resistivity (PTCR) [13] and has been associated to an electrical potential barrier from the presence of a two-dimensional surface layer of acceptor state, e.g., segregation acceptor ions, or adsorbed oxygen at the grain boundaries of the ceramic materials [14]. The results of earlier studies showed that some materials with ABO_3 structure present a V-type resistivity–temperature characteristics [15–17] which was believed to be intrinsic to semiconducting ceramics with ABO_3 structure. Fig. 8 shows the electrical resistivities as a function of temperature between 0 and 40 °C. It, however, shows a semiconductor behavior in the low-temperature region and a metal-like behavior above the transition temperature. Fig. 9 shows the temperature dependence of dielectric constant for $ZnTiO_3$ sintered at 900 °C measured at 1 kHz. The Curie temperature may be located at around 5 °C.

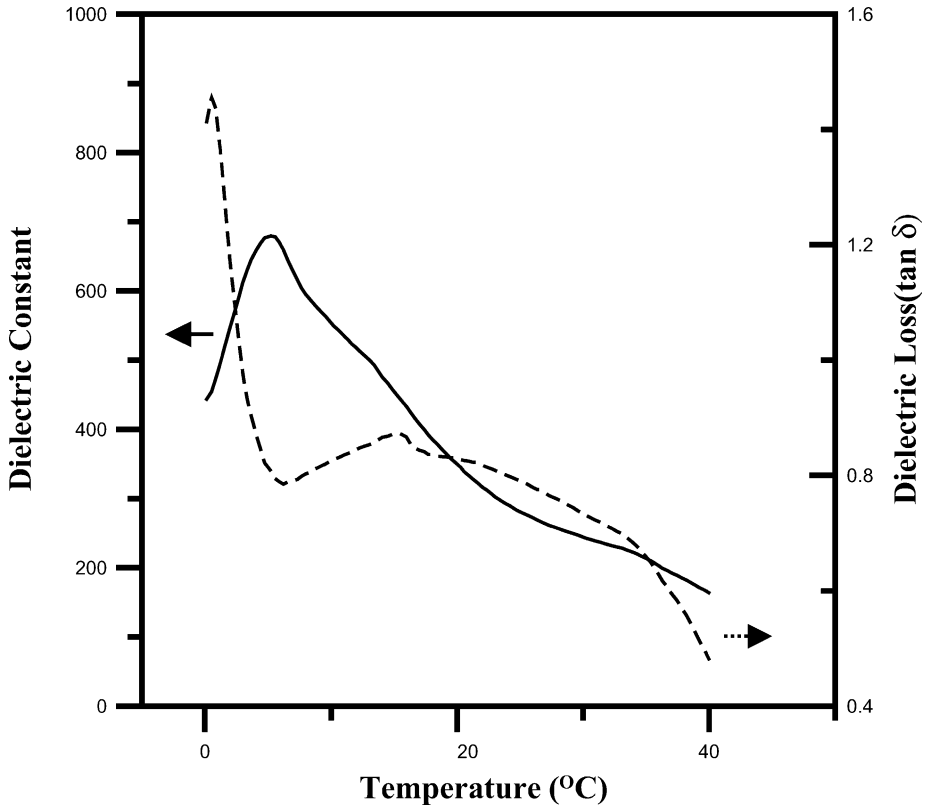

Fig. 9. Temperature dependence of dielectric constant and dielectric loss at 1 kHz for $ZnTiO_3$ sintered at 900 °C.

4. Conclusions

$ZnTiO_3$ powders have been synthesized successfully by solid state reaction. The best conditions for the formation of $ZnTiO_3$ have been found to be 800 °C and 24 h thermal treatment. The grain size of $ZnTiO_3$ powders calcined at various temperatures was about 0.5–1.0 μm. DSC analysis revealed the temperature of $ZnTiO_3$ phase formation to be about 820 °C, the activation energies for the formation of $ZnTiO_3$ phase was about 327.14 kJ/mol and for grain growth was 48.84 kJ/mol. All these figures were higher than for $ZnTiO_3$ synthesized by the sol–gel technique. Like some ferroelectric materials, a PTCR behavior above the transition temperature was observed for $ZnTiO_3$ with Curie temperature at about 5 °C.

Acknowledgements

Authors wish to thank the Nation Science Council of Taiwan for supporting the project (NSC92-2216-E-006-038).

References

[1] F.H. Dulin, D.E. Rase, Phase equilibria in the system ZnO–TiO_2, J. Am. Ceram. Soc. 43 (1960) 125–131.
[2] S.F. Bartram, R.A. Slepetys, Compound formation and crystal structure in the system ZnO–TiO_2, J. Am. Ceram. Soc. 44 (10) (1961) 493–499.
[3] H.T. Kim, S. Nahm, J.D. Byun, Low-fired (Zn, Mg) TiO_3 microwave dielectrics, J. Am. Ceram. Soc. 82 (12) (1999) 3476–3480.
[4] H. Obayashi, Y. Sakurai, T. Gejo, Perovskite-type oxides as ethanol sensors, J. Solid State Chem. 17 (1976) 299–303.
[5] S.F. Wang, M.K. Lu, F. Gu, C.F. Song, D. Xu, D.R. Yuan, S.W. Liu, G.J. Zhou, Y.X. Qi, Photoluminescence characteristics of Pb^{2+} ion in sol–gel derived $ZnTiO_3$ nanocrystals, Inorg. Chem. Commun. 6 (2003) 185–188.
[6] S.F. Wang, F. Gu, M.K. Lu, C.F. Song, D. Xu, D.R. Yuan, S.W. Liu, Photoluminescence of sol–gel derived $ZnTiO_3$:Ni^{2+} nanocrystals, Chem. Phys. Lett. 373 (2003) 223–227.
[7] O. Yamaguchi, M. Morimi, H. Kawabata, K. Shimizu, Formation and transformation of $ZnTiO_3$, J. Am. Ceram. Soc. 70 (1987) c97–c98.
[8] Y.S. Chang, Y.H. Chang, I.G. Chen, G.J. Chai, Y.L. Chai, Synthesis and characteristization of zinc titanate nano-crystal powders by sol–gel technique, J. Cryst. Growth 243 (2002) 319–326.
[9] B.D. Cullity, Elements of X-ray Diffraction, 2nd ed., Addison-Wesley Publishing Company Inc., 1978.
[10] R.L. Coble, Sintering crystalline solids. II. Experimental test of diffusion models in powder compact, J. Appl. Phys. 32 (1961) 793–799.
[11] M. Jarcho, C.H. Bolen, R.H. Doremus, Hydroxyapatite synthesis and characterization in dense polycrystalline form, J. Mater. Sci. 11 (1976) 2027–2035.
[12] H.E. Kissinger, Variation of peak temperature with heating rate in differential thermal analysis, J. Res. Nbs. 57 (1956) 217–221.
[13] J. Daniels, K.H. Härdtl, R. Wernicke, The PTC effect of barium titanate, Philips Tech. Rev. 38 (3) (1978) 73–82.
[14] W. Heywang, Resistivity anomaly in doped barium titanate, J. Am. Ceram. Soc. 47 (1964) 484–490.
[15] Z. Jingchang, L. Longtu, G. Zhilun, A study of V-shape PTC behaviour of $Sr_{0.4}Pb_{0.6}TiO_3$ ceramics, J. Eur. Ceram. Soc. 22 (2002) 1171–1175.
[16] I.C. Ho, S.L. Fu, Effect of reoxidation on the grain-boundary accept-state density of reduced $BaTiO_3$ ceramics, J. Am. Ceram. Soc. 75 (3) (1992) 728–730.
[17] J.G. Kim, W.S. Cho, K. Park, Effect of reoxidation on the PTCR characteristics of porous (Ba, Sr) TiO_3, Mater. Sci. Eng. B 94 (2002) 149–154.